

## de Haas-van Alphen studies in zirconium to 92 kG

P. M. Everett\*

*Department of Physics and Astronomy,  
University of Kentucky, Lexington, Kentucky 40506*  
(Received 15 January 1979)

An investigation of the de Haas-van Alphen effect in Zr has been made using the field-modulation method in fields to 92 kG. Three new branches in the de Haas-van Alphen spectrum have been observed and several previously observed branches have been extended over wider angular ranges. The  $\beta$  and  $\gamma$  branches have been shown to coalesce into a single branch and have been traced throughout all three symmetry planes. The cyclotron mass values have been obtained for this branch at  $\langle 11\bar{2}0 \rangle$  and  $\langle 10\bar{1}0 \rangle$ . The Fermi-surface model of Jepsen, Andersen, and Mackintosh appears to be able to account for the experimental results if it is appropriately modified, particularly in the third and fourth Brillouin zones.

## I. INTRODUCTION

The Zr Fermi surface was first studied experimentally by Thorsen and Joseph<sup>1</sup> who used the pulsed-field technique to 190 kG and established the existence of several branches in the de Haas-van Alphen (dHvA) frequency spectrum. Schirber<sup>2</sup> examined the pressure dependence of these dHvA frequencies along the three symmetry directions and reduced the uncertainties in their values but found no additional frequencies. A study (I) of the transverse magnetoresistance and Hall effect<sup>3</sup> showed that the Zr Fermi surface supports no open orbits in the high-field limit. The mundane character of the magnetoresistance rotation patterns tended to indicate that the Fermi surface is fairly smooth. A dHvA study (II) to 57 kG using the field-modulation technique<sup>4</sup> substantially reduced the uncertainties in the frequency values and detected two previously unknown branches in the dHvA spectrum.

Altmann and Bradley<sup>5</sup> (AB) used the cellular method to perform the first band calculation for Zr. Their Fermi surface is complex, multiply connected, and supports large numbers of open orbits in the single-zone scheme. While several of the dHvA frequency branches can be accounted for in a qualitative way by this Fermi surface, major alterations are required to fit the totality of the presently available data. Loucks<sup>6</sup> performed an augmented-plane-wave calculation for Zr. This Fermi surface differs substantially from that of AB although they can be made similar with appropriate modification of the potentials.<sup>6</sup> While the Loucks Fermi surface is much simpler, it also supports open orbits with both the third and fourth zone sheets intersecting the hexagonal zone plane. It was necessary to pinch off the third zone neck to bring the model into agreement with one branch of the dHvA spectrum that clearly comes from a nearly prolate spheroid. Loucks point-

ed out that this could be accomplished with a reasonable adjustment of the potentials which also removed the fourth zone neck bringing the model into agreement with the magnetoresistance results. Louck's model contains a multiply connected sheet in the fifth zone and some ellipsoids in the sixth zone. All the frequency branches observed in II could be assigned at least qualitatively to Louck's modified Fermi surface although some exacting modifications of the fifth zone sheet were necessary to fit the observed angular dependences. No oscillations were observed that could be assigned to the sixth zone ellipsoids. Jepsen, Andersen, and Mackintosh<sup>7</sup> (JAM) performed a band calculation for Zr using the relativistic linear muffin-tin-orbital method of Andersen.<sup>8</sup> The resulting Fermi surface is similar to that of Loucks in the third and fourth zones, but the Loucks fifth and sixth zone sheets are replaced by two closed, simply connected sheets, one in each zone. The dHvA frequency spectrum of II is also qualitatively accounted for by the JAM Fermi surface if the third zone sheet is closed off in a manner similar to that proposed by Loucks.

It is clear that the entire dHvA spectrum was not observed in II and that more experimental results are needed to guide the theoretical investigations and distinguish between the models. Therefore, new measurements at higher fields were undertaken with an improved dHvA detection system.

## II. EXPERIMENT

The superconducting solenoid used in this investigation was manufactured by American Magnetics, Inc. It is capable of producing 72 kG at 4.2 K and 92 kG and 2 K. The sample holder and detection magnetometer were similar to those used in II and will not be described. However, two important

differences should be noted. The magnet's persistent mode switch was removed, and a current regulated  $1/H$  drive<sup>9</sup> was used to control the magnet power supply. This allowed the solenoid current to be measured directly which improved the accuracy of the dHvA frequency measurements over that of II.<sup>10</sup> The current was calibrated against magnetic field with nuclear magnetic resonance and was monitored with a Fluke differential voltmeter. In addition to being displayed on a strip chart recorder, the dHvA oscillations were recorded digitally on magnetic tape and Fourier analyzed with an IBM 370-165 computing system. The three samples used in II were also used for these measurements.

The dHvA frequency spectrum is shown in Fig. 1. The previously observed  $\beta$ ,  $\gamma$ , and  $\zeta$  branches were extended over substantially wider angular ranges. Additionally, new branches labeled  $\theta$ ,  $\iota$ , and  $\kappa$  were observed. The second harmonics of the  $\alpha$  and  $\beta$  oscillations were observed as well as several sum frequencies presumably produced through magnetic interaction.<sup>11</sup> The individual values of the fundamental frequencies are shown by crosses, and the ranges over which the nonfundamental frequencies were observed are shown by the heavier solid lines. A thin

solid line aids in tracing the  $\iota$  branch through the other branches crossing it. An error in the frequency assignment of II was detected through the Fourier analysis of these data. That portion of what is thought to be a continuous  $\theta$  branch is labeled  $\theta_1$  in the vicinity of  $[0001]$  and lies very close in frequency to  $\gamma$ . The amplitude of the  $\gamma$  branch changes slowly with angle in the immediate vicinity of  $[0001]$ . At  $[0001]$   $\theta_1$  dominates  $\gamma$  by a factor of about 2:1 while  $3^\circ$  away  $\gamma$  is twice as strong as  $\theta_1$ . Since the two frequencies are so close and are beating with both  $\beta$  and  $\alpha$ , they could not be individually detected on the recorder tracings. Thus in II only the dominant oscillation was counted and was assumed to be a single continuous branch. Since the dominant oscillation at  $[0001]$  is  $\theta_1$ , the value listed in Table I of II for  $\gamma$  is actually that of  $\theta_1$ . The  $[0001]$  value for  $\gamma$  could only be obtained from the Fourier expansion, and the uncertainty in its value is relatively large. A  $[0001]$  Fourier spectrum is shown in Fig. 2. The  $\alpha$  and  $\beta$  peaks have been truncated and the scale expanded to show the weaker oscillations. In this spectrum the  $\iota$  peak is just noticeable on the side of a subsidiary maximum of the strong  $\beta$  oscillation. It is more distinct at other orientations. The  $\theta$  and  $\gamma$  peaks are

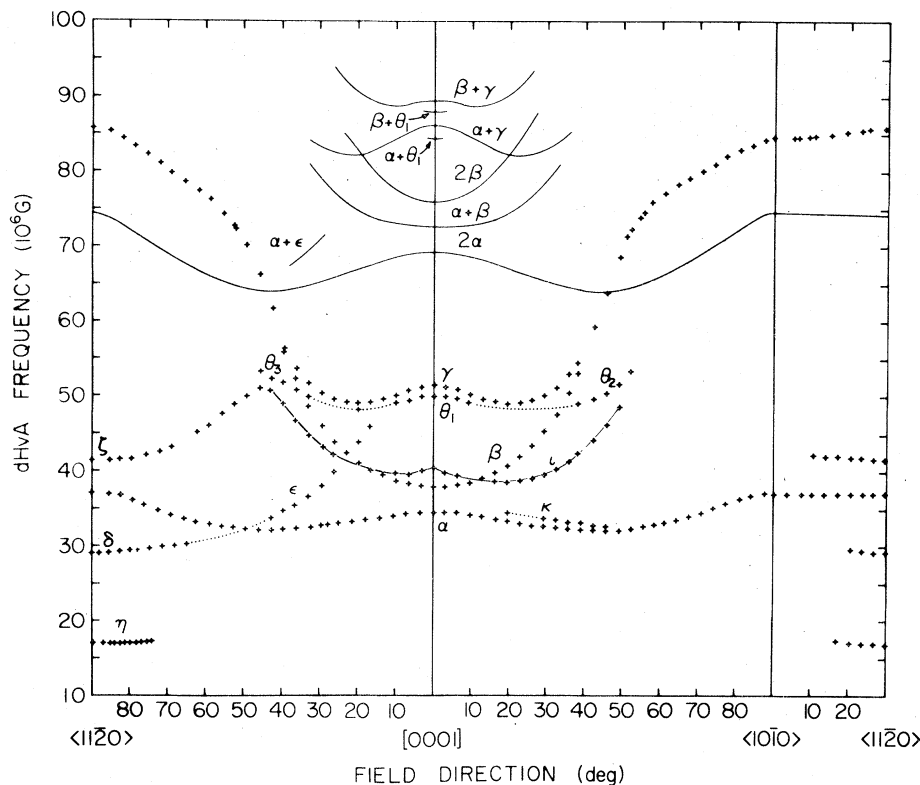


FIG. 1. Collected dHvA frequency values vs magnetic field direction. The measured values of the fundamental frequencies are shown as '+'s, and the ranges over which the second harmonics and sum frequencies were observed are indicated by the heavier solid lines. A thin line is shown to help trace the  $\iota$  branch through the branch crossings. Dotted lines connect data along what are thought to be continuous branches.

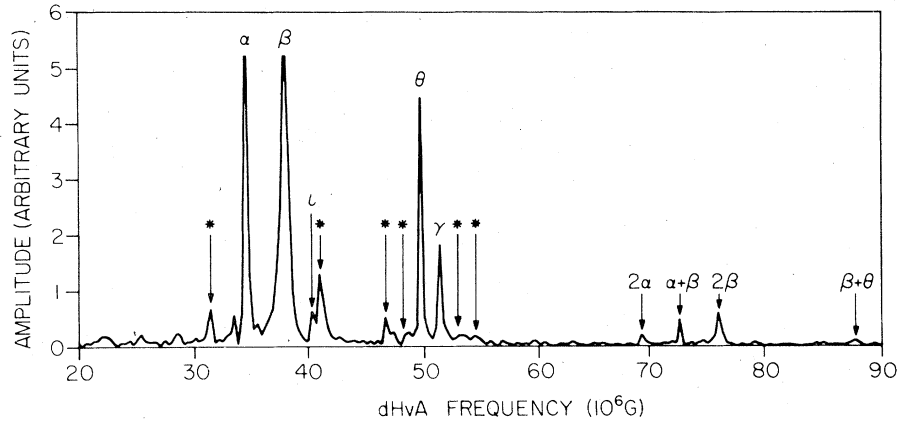


FIG. 2. Fourier spectrum at [0001]. The  $\alpha$  and  $\beta$  peaks have been truncated in order to expand the scale. In these units the heights of the  $\alpha$  and  $\beta$  peaks are 11.7 and 28.6, respectively. The field sweep contained approximately 150  $\theta$  oscillations at a density of 50 points per oscillation. The peaks marked with an asterisk are the first subsidiary maxima of the stronger oscillations. The weaker oscillations were enhanced in other spectra by adjusting the amplitude of the modulation field.

clearly displayed. The Fourier spectra were taken at approximately  $3^\circ$  intervals, and the  $\theta$ - $\gamma$  assignment was made by assuming smoothly varying angular dependences. The symmetry axis values for the dHvA frequencies are shown in Table I. Aside from the  $\gamma$ - $\theta$  assignment there are only slight differences from those given in II. The mass of the  $\beta$ - $\gamma$  oscillation was measured at the  $\langle 11\bar{2}0 \rangle$  and  $\langle 10\bar{1}0 \rangle$  axes from the temperature dependence of oscillation amplitude. These mass values are also given in Table I.

One of the main reasons for undertaking these measurements was to trace the  $\beta$  and  $\gamma$  branches over a wider angular range. It appeared from II that  $\beta$  and  $\gamma$  were blending as though they were orbits on the same sheet of Fermi surface. However, this was not definitely shown to be the case. Also, if  $\beta$  and  $\gamma$

did result from central and noncentral orbits on the same simply connected sheet of the Fermi surface it appeared questionable whether the sheet would close inside the hexagonal zone face. The  $\beta$  and  $\gamma$  frequencies have been shown to blend into a single branch and have been traced throughout all three symmetry planes. The only questions that remain are which orbit is central and whether the sheet is closed through magnetic breakdown. An expanded plot of the  $\beta$ - $\gamma$  branch in the basal plane is shown in Fig. 3. Since the branch varies only slightly, the dHvA data were inverted by assuming that the sheet supporting these oscillations is a cylinder of revolution about the  $c$  axis. This was done twice by assigning in turn the  $\beta$  and  $\gamma$  branches to be the central orbit. An 18th-degree polynomial was fitted to the branch in ques-

TABLE I. dHvA frequency and cyclotron mass values at the symmetry axes.

oscillation	axis	dHvA frequency (MG)	cyclotron mass (in units of free-electron mass)
$\alpha$	$\langle 10\bar{1}0 \rangle$	$37.28 \pm 0.04$	
	$\langle 11\bar{2}0 \rangle$	$37.15 \pm 0.04$	
	[0001]	$34.58 \pm 0.04$	
$\beta$	[0001]	$38.00 \pm 0.04$	
$\gamma$	[0001]	$51.61 \pm 0.10$	
$\beta$ - $\gamma$	$\langle 10\bar{1}0 \rangle$	$84.49 \pm 0.06$	$2.31 \pm 0.03$
	$\langle 11\bar{2}0 \rangle$	$85.73 \pm 0.05$	$2.62 \pm 0.03$
$\delta$	$\langle 11\bar{2}0 \rangle$	$29.04 \pm 0.03$	
$\zeta$	$\langle 11\bar{2}0 \rangle$	$41.32 \pm 0.04$	
$\eta$	$\langle 11\bar{2}0 \rangle$	$16.88 \pm 0.02$	
$\iota$	[0001]	$40.52 \pm 0.08$	
$\theta$	[0001]	$49.88 \pm 0.05$	

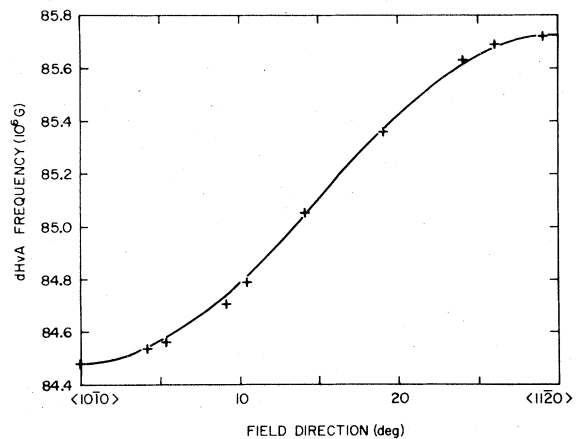


FIG. 3. Expanded plot of the  $\beta$ - $\gamma$  frequency values in the basal plane. The solid line is a half-cycle cosine fitted to the symmetry axis values and is shown for comparison purposes.

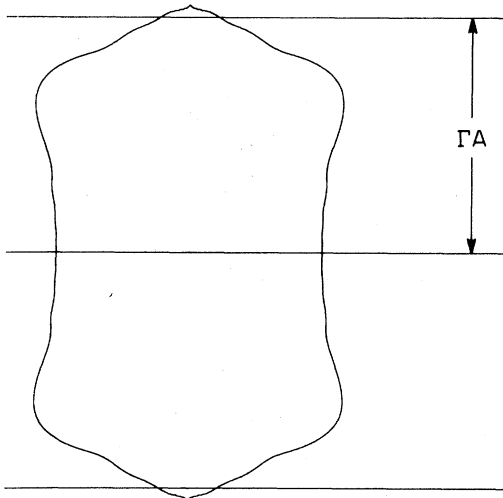


FIG. 4. Cross section of the surface of revolution fit to the  $(10\bar{1}0)$   $\beta$  data.  $\Gamma A$  is the half height of the Brillouin zone.

tion to smoothly interpolate equally spaced frequency values from  $[0001]$  to  $\langle 11\bar{2}0 \rangle$ .<sup>12</sup> The sheet was approximated by 2000 coaxial circular disks stacked one on the other. Starting from  $[0001]$  1000 successive frequency values along the branch were used to determine the radius and thickness of each disk in turn so that the central cross section of the sheet corresponded to the frequency data. The sheet of the Fermi surface determined in this way by assuming that  $\beta$  is the central orbit is shown in Fig. 4. The angular dependence of the central cross section is shown as a dHvA frequency in Fig. 5 with the  $\beta$  data. The fit is to within 0.5% throughout the  $90^\circ$  interval. The noncentral extremal cross section of this sheet was traced and is also shown as a dHvA frequency in Fig. 5 with the  $\gamma$  which were not used in the calculation. By inverting the  $\beta$  data a noncentral extremal orbit is predicted that closely fits the  $\gamma$  data. The predicted branch does drop below the  $\gamma$  data by slightly more than 1% about  $18^\circ$  from  $[0001]$ . However, this is well within the error in the inversion that is expected from the basal plane anisotropy of the true Fermi surface. The center of the maximal orbit moves toward the center of the sheet with increasing angle until it reaches it as the two branches coalesce. From Fig. 4 it can be seen that the sheet obtained from this inversion extends through the hexagonal zone face as though the sheet were normally open and were closed by inserting a cap through magnetic breakdown. However, the volume of  $k$  space contained within this cap is very small, and the cap's existence is within the uncertainty of the inversion. It is clear that the end of the sheet lies close to the zone face. The sheet obtained by assuming  $\gamma$  to be the central orbit is shown in Fig. 6 and the extremal

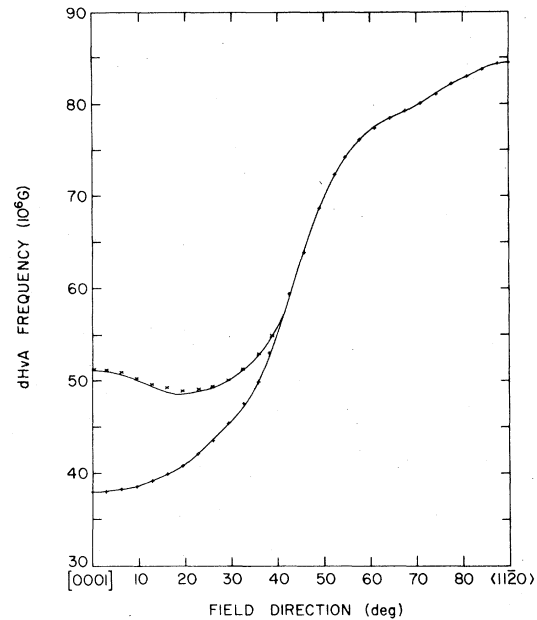


FIG. 5. Extremal cross sections shown as dHvA frequencies vs field direction for the Fermi-surface sheet shown in Fig. 4. The solid lines trace the extremal cross sections. The  $\beta$  data used in the inversion are shown as +'. The  $\gamma$  data, shown as x's, were not used in the inversion and are shown for comparison with the noncentral cross section. The agreement of the lower line with the  $\beta$  data shows the accuracy of the polynomial fit.

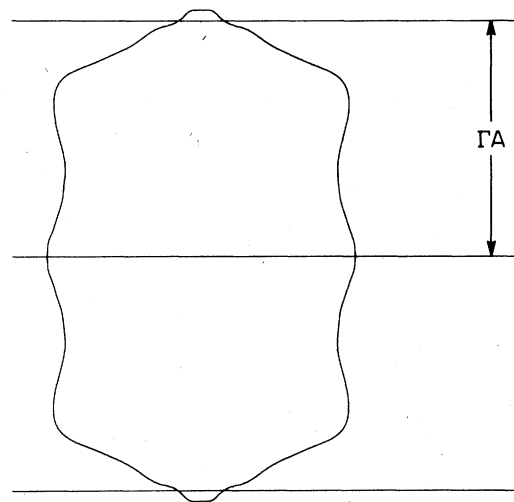


FIG. 6. Cross section of the surface of revolution fit to the  $(10\bar{1}0)$   $\gamma$  data.  $\Gamma A$  is the half height of the Brillouin zone.

orbits obtained from it are shown in Fig. 7. The sheet supports the central  $\gamma$  orbit and noncentral maximal and minimal orbits. The minimal orbit is 5% larger than that appropriate for  $\beta$  along [0001]. With increasing angle the center of the noncentral maximal orbit moves toward the center of the sheet, and the center of the minimal orbit moves away from the sheet center. At slightly more than twenty degrees from [0001] the two noncentral orbits coalesce and cease to be extremal, which does not correspond to the observed union of the  $\beta$  and  $\gamma$  branches. Since the inversion with the  $\beta$  orbit as central predicts the  $\gamma$  branch so well it seems reasonable that this choice is correct. Also the Fermi surface of Fig. 4 fits the general amplitude behavior of the  $\beta$  and  $\gamma$  branches.<sup>13</sup>

The  $\theta$  branch was only observed over three isolated regions. Around [0001] the oscillation was quite strong and easily observed. Away from [0001] the amplitude decreased, and the  $\theta$  oscillation could not be extracted from the tail of the  $\gamma$  peak in the Fourier spectrum. However, inflections on the low-frequency tail did support the existence of the oscillation between  $\theta_1$  and  $\theta_2$  and  $\theta_3$ . The dotted lines connecting the three  $\theta$  branches in Fig. 1 follow these inflections. The  $\iota$  branch was traced through the Fourier expansion over a connected range except

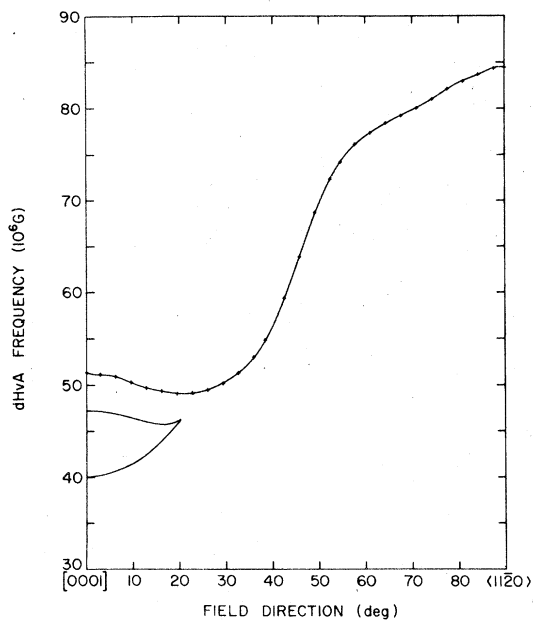


FIG. 7. Extremal cross sections shown as dHvA frequencies vs field direction for the Fermi-surface sheet shown in Fig. 6. The solid lines trace the extremal cross sections. The two noncentral extremal cross sections cease to exist at slightly more than 20° from [0001]. The  $\gamma$  data to which the fit was made are shown as '+'s.

where it crossed stronger branches. It appears that  $\theta$  and  $\iota$  are blending together as though they are orbits on the same sheet of the Fermi surface. However, the branches could not be traced far enough to establish this.

During part of one data taking run the detection system and magnet control unit were particularly stable. The peaks in the Fourier spectrum were unusually sharp and an oscillation slightly higher in frequency than  $\alpha$  was clearly visible. This branch of the dHvA spectrum labeled  $\kappa$  was observed in the (11 $\bar{2}$ 0) plane from 19.5 to 46° from [0001]. A Fourier spectrum 42.5° from [0001] containing the  $\kappa$  peak is shown in Fig. 8. The detection system acted in a more normal fashion during the earlier part of this run when the data from [0001] out to 19.5° were taken and the later part beyond 46°. The strong  $\alpha$  peak in the Fourier spectrum was broader, washing out the  $\kappa$  peak. This was also true for the two field sweeps at 22.7 and 26.0° and for the entire run in the (10 $\bar{1}$ 0) plane. The possibility that  $\alpha$  and  $\kappa$  are central and noncentral orbits on the same simply connected, closed sheet of the Fermi surface was considered. The  $\alpha$  data were inverted using the same procedure for  $\beta$  and  $\gamma$ . The resulting surface is the same as that shown in Fig. 5(a) of II and does not support a noncentral orbit that could account for  $\kappa$ . It is possible that  $\alpha$  is the noncentral and  $\kappa$  is the central orbit. While there is insufficient  $\kappa$  data to allow for a truly meaningful inversion of this branch, it was roughly extrapolated to [0001] and blended into the  $\alpha$  branch around 55° from [0001]. The inversion of this extended  $\kappa$  branch also yielded a Fermi surface that supports only a single extremal orbit. Also it seems highly unlikely that the central orbit could be so very much weaker (~5%) than the noncentral orbit. Thus it appears that  $\alpha$  and  $\kappa$  come from different Fermi-surface sheets.

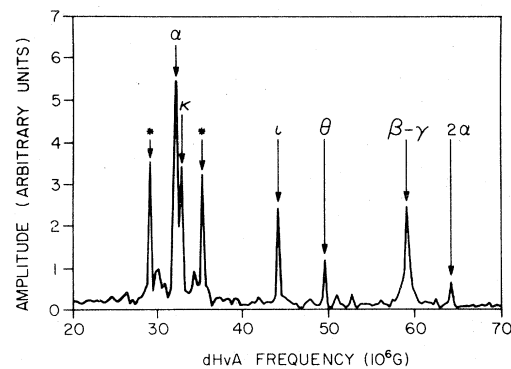


FIG. 8. Fourier spectrum 42.5° from [0001] in the (11 $\bar{2}$ 0) plane. The  $\alpha$  peak has been truncated in order to expand the scale, and in these units its height is 70.1. The peaks marked with an asterisk are the first subsidiary maxima of the  $\alpha$  oscillation.

The amplitude of the  $\delta$  oscillation decreases rapidly and steadily going from  $\langle 11\bar{2}0 \rangle$  toward  $[0001]$ . At  $\langle 11\bar{2}0 \rangle$  the  $\delta$  amplitude is more than half that of the  $\alpha$  oscillation, while  $10^\circ$  away it is no more than 10% of the  $\alpha$  amplitude. The oscillation was traced in the Fourier spectrum through an angular range of  $25^\circ$  from  $\langle 11\bar{2}0 \rangle$ . At this orientation the weak  $\delta$  oscillation blended into a subsidiary maximum of the  $\alpha$  oscillation. Continuing toward the basal plane inflections were observed on the  $\alpha$  peak indicating the continued existence of the  $\delta$  oscillation, but the oscillation itself was not isolated. Just after the  $\delta$  and  $\alpha$  branches appear to cross, the amplitude of what has been called the  $\epsilon$  branch increased dramatically. The slopes of the  $\delta$  and  $\epsilon$  branches match very well. This combined with the inflections that move through the  $\alpha$  peak are strong evidence that  $\delta$  and  $\epsilon$  are actually portions of the same dHvA branch. The branch was traced to within  $17^\circ$  of  $[0001]$  where the amplitude decreased smoothly to an unobservable level.

### III. FERMI-SURFACE MODELS

An appropriately altered Loucks model can account for the experimental results of I and II. The modification proposed by Loucks to pinch off the third and fourth zone necks to account for the  $\alpha$  oscillation and remove the open orbits leaves a fourth zone sheet that resembles that shown in Fig. 6. If instead this sheet were centrally waisted it would be very much like that shown in Fig. 4, in both size and shape, and could account for the  $\beta$  and  $\gamma$  oscillations. A modified fifth zone sheet can account for the  $\eta$ ,  $\zeta$ , and unconnected  $\delta$  and  $\epsilon$  oscillations. It supports several other extremal orbits, two of them perpendicular to  $[0001]$ . However, both are too small, as is the orbit on the sixth zone ellipsoids, to account for either  $\iota$  or  $\theta$ . It is not clear where the  $\kappa$  orbit can be assigned in this model.

The third and fourth zone sheets of the JAM model are very much like those of Loucks, and the above discussion concerning them is for the most part applicable. The major difference is that the modification JAM propose for closing the third zone sheet does not close the fourth zone sheet and leaves a smaller nearly isotropic sheet in the third zone, in addition to the larger one assigned to  $\alpha$ . No oscillation has yet been observed that can be assigned to this smaller sheet. Specific searches were made for it along all three symmetry axes, but the lack of observation should not be interpreted as proof of nonexistence. The field-modulation magnetometer used for these measurements was not particularly sensitive to frequencies this low (a few MG) since the amplitude of the modulation field was limited to 80 G.<sup>14</sup> A search using a torque magnetometer would be much more convincing. JAM do not propose a

modification for closing the fourth zone sheet, and one possibility is that it is closed by the smaller third zone sheet through magnetic breakdown. This would be consistent with the result of the inversion scheme except that the size of the intersection with the zone face would have to be reduced and the fourth zone sheet waisted. With these changes the third and fourth zone sheets are able to account for the  $\alpha$ ,  $\beta$ , and  $\gamma$  oscillations.

The simply connected fifth zone sheet in the JAM model supports an extremal orbit that they have assigned to  $\zeta$ . In the model this orbit is slightly smaller at  $\langle 10\bar{1}0 \rangle$  than it is at  $\langle 11\bar{2}0 \rangle$ . The  $\zeta$  branch has not been extended to  $\langle 10\bar{1}0 \rangle$  and in fact rises slightly leaving  $\langle 11\bar{2}0 \rangle$ . However, this is not sufficient reason to doubt the orbit assignment. The sheet also supports two extremal orbits perpendicular to  $[0001]$  that are almost the size needed to account for  $\iota$  and  $\theta$ . These two orbits are central and noncentral and would coalesce as the orbit normals move toward the basal plane. The symmetry axis values for  $\zeta$ ,  $\iota$ , and  $\theta$  agree with the sizes of the orbits supported on JAM's fifth zone sheet to better than 10% which is indeed encouraging. JAM assigned the  $\eta$  oscillation to an orbit on their sixth zone sheet. While the orbit size corresponds to a dHvA frequency only half that observed, the energy band producing this sheet is fairly flat in the vicinity of the Fermi level. A minor shift in the Fermi level might appropriately adjust the size of the sheet, and the disagreement with the dHvA frequency should probably not be considered significant. Also, such an orbit fits the angular dependence of  $\eta$  shown in II. This orbit might account for  $\kappa$  as well; i.e.,  $\eta$  and  $\kappa$  might be portions of the same dHvA branch. The model supports an  $[0001]$  orbit that fits well with the rather dubious extension of the  $\kappa$  branch.

There remain only the  $\delta$  and  $\epsilon$  oscillations. JAM are not definite as to the orbit assignment on their Fermi surface, but it seems most likely that  $\zeta$  corresponds to the central orbit on the fifth zone-hole sheet. Clearly such an extremal orbit must exist, at least along  $\langle 10\bar{1}0 \rangle$ . JAM show only cuts of their Fermi surface so it is not possible to construct it in detail. It does appear possible that a noncentral minimal extremal orbit along  $\langle 11\bar{2}0 \rangle$  somewhat smaller than the central orbit exists in the valley between the lips and the humps on both top and bottom of the fifth zone sheet. Rotating the orbit normal toward  $\langle 10\bar{1}0 \rangle$  the orbit could exist for a time and then cease to be extremal. Rotating the orbit normal toward  $[0001]$  the width of the band of extremal orbits would probably decrease as the orbit went up the sides of the lip and humps decreasing the observed signal. With increasing angle the orbit would go over the end of the lip and the tops of the humps almost simultaneously markedly increasing the observed signal. Continuing toward  $c$  the orbit

would fall down the outside of the lip and cease to be extremal somewhere around  $20^\circ$  from  $c$ . This analysis is built on a rather crude reproduction of the JAM Fermi surface. Since JAM do not consider this possibility, the orbits described may not actually be extremal, at least in their present model. However, such a possibility does describe very well both the frequency and amplitude behavior of a continuous  $\delta$ - $\epsilon$  branch. However, it does seem fortuitous that the complex shape of this orbit on the JAM Fermi surface would compensate in such a way as to give the nearly secant angular dependence of  $\delta$  which is shown in II.<sup>15</sup> The value of the  $\delta$  frequency at  $\langle 11\bar{2}0 \rangle$  is within the experimental uncertainty of the average of the  $\eta$  and  $\zeta$  values. Primarily because of this JAM assigned the  $\delta$  orbit to magnetic breakdown connecting the  $\eta$  and  $\zeta$  orbits. This would seem unlikely in view of the wide angular range over which the branch has been observed. Also, it is not clear that the angular dependences of the  $\eta$  and  $\zeta$  branches shown in II can be combined to give the angular dependence of  $\delta$ .

The fifth and sixth zone sheets in the JAM model offer much better agreement with the experimental results than do the corresponding sheets in the Loucks model. The  $\iota$ ,  $\theta$ , and  $\kappa$  oscillations cannot be easily assigned to orbits on the Loucks Fermi surface while they can on that of JAM. Rather exacting modifications of the shape of the Loucks fifth zone sheet are required to account for the angular dependences of the  $\delta$ ,  $\zeta$ , and  $\eta$  oscillations while this is required on the JAM Fermi surface only for the  $\delta$  os-

cillation. Except for  $\eta$  the sizes of all the orbits on JAM's fifth and sixth zone sheets agree with the experimental results to better than 10% while the oscillations that can be assigned to orbits on the Loucks Fermi surface are generally 40% smaller than those predicted by the model. Also it appears that oscillations have been observed that can be assigned to all of the extremal orbits on JAM's fifth and sixth zone sheets, at least over part of their angular ranges. The third and fourth zone sheets in both models must be substantially altered, and it is not clear what effect this will have on the fifth and sixth zone sheets. However, since the shapes of both the third and fourth zone sheets have been determined experimentally, it should now be possible to adjust the calculations to give realistic representations of the Zr band structure. Two related questions which this experiment has not been able to answer are the intersection or nonintersection of the fourth zone sheet with the hexagonal zone face and the size of the band gap across this face. If the fourth zone sheet is closed by magnetic breakdown the magnetoresistance results of I indicate that the band gap must be very small.<sup>16</sup>

#### ACKNOWLEDGMENT

The support of the Research Corporation is gratefully acknowledged. The author wishes to thank Professor C. G. Grenier and Professor R. G. Goodrich for loaning their magnet power supply which was used in this investigation. The support of Dr. D. R. Collins is also gratefully acknowledged.

\*Present address: Texas Instruments, Inc., Dallas, Texas 75265.

<sup>1</sup>A. C. Thorsen and A. S. Joseph, Phys. Rev. **131**, 2078 (1963).

<sup>2</sup>J. E. Schirber, Phys. Lett. A **33**, 172 (1970).

<sup>3</sup>P. M. Everett, Phys. Rev. B **6**, 3553 (1972).

<sup>4</sup>P. M. Everett, Phys. Rev. B **6**, 3359 (1972).

<sup>5</sup>S. L. Altmann and C. J. Bradley, Phys. Rev. **135**, A1253 (1964); Proc. Phys. Soc. London **92**, 764 (1967).

<sup>6</sup>T. L. Loucks, Phys. Rev. **159**, 544 (1967).

<sup>7</sup>O. Jepsen, O. Krogh Andersen, and A. R. Mackintosh, Phys. Rev. B **12**, 3084 (1975).

<sup>8</sup>O. Krogh Andersen, Phys. Rev. B **12**, 3060 (1975).

<sup>9</sup>P. M. Everett, Rev. Sci. Instrum. **48**, 1143 (1977).

<sup>10</sup>The superconducting magnet used in II contained a persistent mode switch. The total power supply current was monitored and that portion of the current flowing through the persistent mode switch, depending on the sweep rate, solenoid inductance, and switch resistance, had to be estimated. This estimate introduced an additional uncertainty into the results of II which is not present in these results. Also the NbTi multifilamentary wire used for this magnet retained a residual field from trapped flux never in excess of 10 G, while the magnet used in II retained residual fields as large as 100 G.

<sup>11</sup>D. Shoenberg, Philos. Trans. R. Soc. London Sect. A **255**,

85 (1962).

<sup>12</sup>As shown in Figs. 5 and 7 the polynomial fits the data quite accurately. A spline procedure was also attempted, but the results were far less satisfactory with the fit being choppy.

<sup>13</sup>Inversions were also made using both the  $\beta$  and  $\gamma$  branches in the  $\langle 11\bar{2}0 \rangle$  plane. Differences in the  $\beta$ - $\gamma$  frequency values between the two planes occur only near the basal plane, and the sheets obtained in this way differ from those shown in Figs. 4 and 6 only in minor details. The value used for the hexagonal lattice vector to obtain the Brillouin-zone dimension was  $c = 5.141 \text{ \AA}$ .

<sup>14</sup>Vibration resulting from the interaction between the magnet and the modulation solenoid tended to break the samples loose from their mounting for modulation levels above this.

<sup>15</sup>Cross section of a straight-sided cylinder of any shape increases as the secant of the angle between the normal to the cross section and the cylinder axis.

<sup>16</sup>Transverse magnetoresistance results of I exhibit quadratic field dependence above a few hundred gauss for all field directions with the current along each of the three symmetry directions. This would appear to eliminate any possibility of open orbits above these fields at least to within the sample orientation uncertainty of less than  $1^\circ$ .